

# ***AutArch*: An AI-assisted workflow for object detection and data collection from archaeological catalogues**

Kevin Klein<sup>1,2\*</sup>, Alyssa Wohde<sup>3</sup>, Alexander V. Gorelik<sup>1,2</sup>, Volker Heyd<sup>4</sup>, Ralf Lämmel<sup>5</sup>, Yoan Diekmann<sup>1#</sup>, Maxime Brami<sup>1#\*</sup>

# These authors contributed equally.

\* Corresponding authors: Kevin Klein ([kkevin@students.uni-mainz.de](mailto:kkevin@students.uni-mainz.de)), Maxime Brami ([mbrami@uni-mainz.de](mailto:mbrami@uni-mainz.de))

## **Affiliation**

<sup>1</sup>Palaeogenetics Group, Institute of Organismic and Molecular Evolution (iomE), Johannes Gutenberg University Mainz, Mainz, Germany.

<sup>2</sup>Vor- Und Frühgeschichtliche Archäologie, Institut Für Altertumswissenschaften, Johannes Gutenberg University Mainz, Mainz, Germany.

<sup>3</sup>University of Koblenz, Koblenz, Germany

<sup>4</sup>Department of Cultures / Archaeology, University of Helsinki, Helsinki, Finland

<sup>5</sup>Software Languages Team, University of Koblenz, Koblenz, Germany

## **Abstract**

The *context* of this paper is the creation of large uniform archaeological datasets from heterogeneous published resources, such as find catalogues – with the help of AI and Big Data. The paper is concerned with the *challenge* of consistent assemblages of archaeological data. We cannot simply combine existing records, as they differ in terms of quality and recording standards. Thus, records have to be recreated from published archaeological illustrations. This is only a viable path with the help of automation. The *contribution* of this paper is a new workflow for collecting data from archaeological find catalogues available as legacy resources, such as archaeological drawings and photographs in large unsorted PDF files; the workflow relies on custom software (*AutArch*) supporting image processing, object detection, and interactive means of validating and adjusting automatically retrieved data. We integrate artificial intelligence (AI) in terms of neural networks for object detection and classification into the workflow, thereby speeding up, automating, and standardising data collection. Objects commonly found in archaeological catalogues – such as graves, skeletons, ceramics, ornaments, stone tools and maps – are detected. Those objects are spatially related and analysed to extract real-life attributes, such as the size and orientation of graves based on the north arrow and the scale. We also automate recording of geometric whole-outlines through contour detection, as an alternative to landmark-based geometric morphometrics. Detected objects, contours, and other automatically retrieved data can be manually validated and adjusted (via *AutArch*'s graphical user interface). We use third millennium BC Europe (encompassing cultures such as 'Corded Ware' and 'Bell Beaker', and their burial practices) as a 'testing ground' and for evaluation purposes; this includes a user study for the workflow and the *AutArch* software.

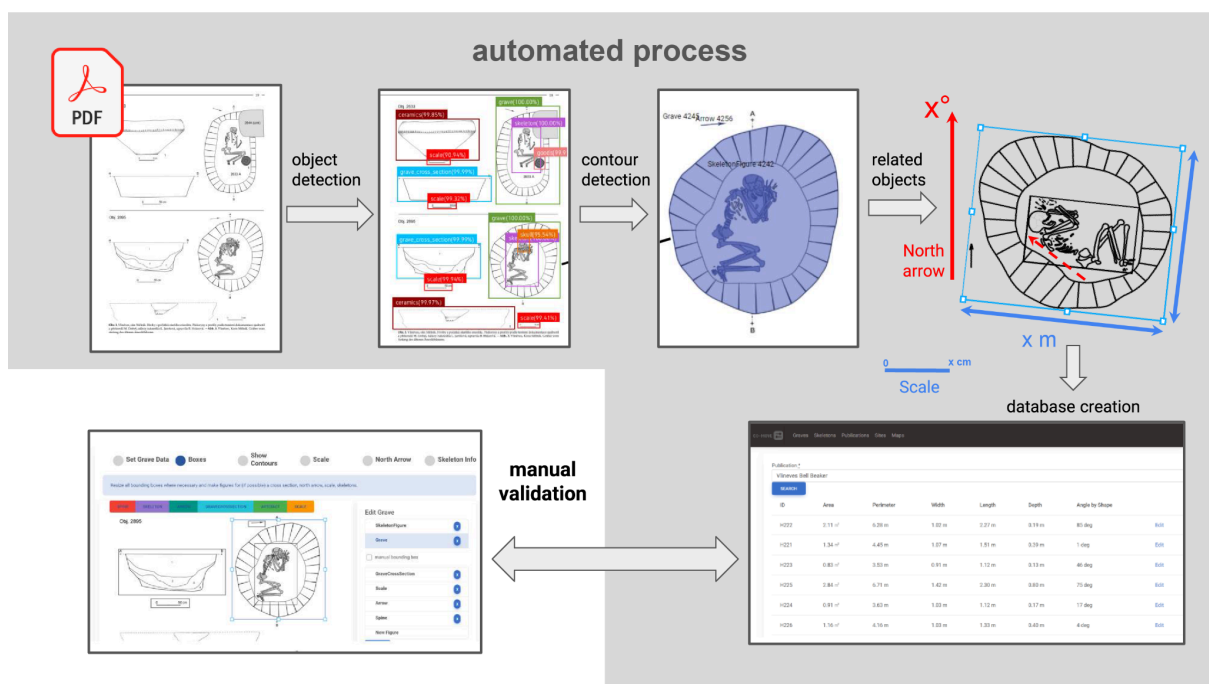
# Keywords

Archaeology, Burials, Artificial Intelligence (AI), Object Detection, Deep Learning, Geometric Morphometrics, AutArch

# Highlights

- Automating archaeological data collection using legacy resources
- Fast and standardised recording for Big Data archaeology
- Contour detection and encoding allowing formal analyses of shapes

# Graphical Abstract



Graphical Abstract. Overview of the AI-assisted workflow (here: Corded Ware site of Vliněves <sup>1</sup>, Czech Republic).

# Video

A video demonstrating the key aspects of the AutArch workflow and software can be downloaded at this address: <https://seafilerp.net/f/50ce9cc0771f4afc9cd0/>

# 1 Introduction

## **Context: *AI and Big Data in Archaeology***

The use of Artificial Intelligence and Big Data models in scientific and commercial applications surged in popularity in recent years. Advances in deep learning, for instance, have enabled users to solve complex image processing problems. These new approaches are often argued to be the next frontier<sup>2</sup> in archaeology, with attempts to consolidate all archaeological datasets into single databases already on the horizon (e.g., Big Interdisciplinary Archaeological Database or BIAD: <https://biadwiki.org/>). In this paper, we apply AI and image processing complemented by a workflow to automated recording in archaeological catalogues.

## **Challenge: *Consistent assemblages of archaeological data***

When aiming at such assemblages, we cannot rely on and integrate existing records. The desired consistency of the assemblages would require the used records to be of comparable quality and to adhere to the same recording standards, which is hardly ever the case in archaeology. ‘Starting all over’ and to identify, characterise, and *manually* record data using published archaeological illustrations would be a prohibitively time-consuming, repetitive and error-prone task – if not assisted by automation, which is however not yet available in archaeology. In the following, we discuss this challenge in more detail.

While the benefits of integrating information from thousands of archaeological PDFs released to date are obvious, there are significant hurdles. Screening thousands of pages of text and images to locate relevant content is a time-consuming and repetitive task; data can be scattered across many parts of the document; papers can be written in different languages and alphabets; various conventions for describing attributes such as the size and orientation of graves apply, so that mere collation of data from published tables results in inconsistent datasets. Using Computer-Assisted Design (CAD) or drawing software products to manually re-measure objects based on published drawings is tedious and prone to error. Therefore, large-scale assembly of uniform (‘sound’) data from a variety of sources is rarely possible in practice.

The lack of unified drawing standards in archaeology especially complicates data comparison across publications. Measuring the width, length and depth of a three-dimensional object, such as a burial pit, for instance, might be expected to yield consistent results independent of author and publication; yet, there are multiple ways to describe objects in archaeology, particularly for irregular shapes. Archaeological site manuals<sup>3</sup> rarely provide guidelines on how to measure non-symmetrical objects such as graves. And while some authors show how the length was measured by drawing a line through the grave<sup>e.g. 4,5</sup>, the width is rarely indicated in the same manner. Even if this information was transparently reported, harmonising measurement conventions would remain a challenge. Reporting the orientation of skeletons in graves is fraught with even more difficulties<sup>6</sup>. The orientation of graves is rarely given in degrees, and when it is, different methods apply, often confusing the orientation of the skeleton with the orientation of the grave cut. In sum, there is no guarantee that reported measurements of spatial objects can be compared across different publications.

## Contribution: *An AI-assisted workflow for data collection*

In this paper, we present *AutArch*, an AI-assisted workflow (and accompanying software) that allows fast, accurate and uniform identification and analysis of objects in unsorted PDF documents.

Previous archaeological approaches leveraging AI have often addressed narrowly focused research questions, for example, classification of artefacts and ecofacts<sup>7-11</sup>, predicting the dating of sites<sup>12</sup>, or interpretation of high-resolution survey images<sup>13-15</sup>. Despite archaeology's traditional emphasis on typological and geometric morphometric approaches<sup>16</sup>, published resources such as archaeological drawings and photographs in illustrated catalogues have remained underutilised<sup>17</sup>.

The process of extracting geometric shapes from publications is starting to be semi-automated for specific artefact classes, such as arrowheads, but the images still need to be prepared for the extraction of artefact outlines<sup>18,19</sup>. *AutArch* provides a general solution that increases the usefulness of published resources by making their content immediately available to archaeologists as data in a well-defined format.

## Testing Ground: *Third Millennium BCE Europe*

Due to the 'messy'<sup>20</sup>, but to some extent repetitive nature of the archaeological record of 3rd millennium BCE Europe, this period provides an interesting testing ground for innovative approaches to data collection and using AI in particular. Tens of thousands of graves and grave inventories have been ascribed to this period. The findings are frequently reported in the form of drawings and photographs accompanied by descriptions written following a variety of professional standards and in different languages.

Historically, archaeological assemblages have been grouped into archaeological 'cultures', based on different classes of attributes, making comparison difficult. Southeast European 'Yamnaya' assemblages, for instance, are defined after a specific type of burial, Russian 'Yama', i.e. 'pit'-graves<sup>21,22</sup>; North-Central European 'Corded Ware' assemblages are characterised by a specific ceramic decoration<sup>23</sup>; Western European 'Bell Beakers' are named after the shape of the ceramic vessels found in graves<sup>24,25</sup>. These attributes sometimes appear together. For instance, All Over Cord (AOC) Beakers have cord impressions<sup>26</sup>. While many studies have dealt with variability in the funerary record, most are still based on the simplest possible attribute dimension: its presence or absence.

Third millennium BC Europe appears to be a strong candidate for the challenge of developing an automated workflow that requires only minimal input from researchers to digitise large datasets recording rich, numerical annotation. On this testing ground, we evaluate the research results along several dimensions; object detection is evaluated in terms of standard metrics; the workflow is evaluated by means of metrics quantifying automated versus manual steps for (a subset of) our dataset; correctness and productivity (usability) of the workflow, as supported by the *AutArch* software, is evaluated by a user study, which also covers comparison with standard practices (such as *Inkscape* for measuring graves).

## Online Resources

The paper is complemented with online resources to better support reproducibility of the reported research. We use a public GitHub repository (<https://github.com/kevin-klein/autarch-material>) to make sure that we can keep all 'materials' (datasets) and accompanying software and AI models up-to-date and well-documented along the publication process and also past publication in response to interaction with interested parties. In the repository, we provide the following assets:

- *The AI training datasets presented in Section 2.2* – due to copyright restrictions, we cannot include the underlying publications (or the images of graves therein or the objects therein such as skeletons and north arrows), but we provide a dump of data extracted (detailing data summarised in the paper) and all labelling data used for training. Interested parties may use the original documents to train the same AI model or a different one, using comparable publications.
- *The AI model presented in Section 2.1* – we provide a usable AI model that can be used to perform object detection and other steps of our workflow on the same (if available) or any suitable publications. To this end, we also release scripts (‘software’) to enable use of the model.
- *A database of collected graves used in this publication* - we provide the data collected from a range of publications in the form of a database dump used for validation purposes in Section 4 and to create the figures in Section 3.
- *The evaluation of object detection, workflow, and usability in Section 4* – the repository provides the raw data in the form of several spreadsheets used for the discussion in Section 4.

## 2 Materials and Methods

We provide an overview of *object detection* as the central method, and discuss the materials underlying the reported research, namely *datasets for graves and objects therein*.

### 2.1 Object Detection

We first describe the general setup (method) of object detection used by us; we then also get into the specifics of object detection in the sense of processing legacy resources (PDF files) containing images of graves.

#### 2.1.1 General Object Detection Setup

Our software realises object detection by means of a ‘deep learning’ approach – in the sense of artificial neural networks (ANNs).

A brief summary of the internals of ANNs is provided here for non-specialized readers. ANNs are mathematical function networks that can be thought of as layers of artificial neurons – also known as Perceptrons or Nodes. Neurons have one or several inputs with associated weights, a bias- and an activation function. For simple linear layers, each input is multiplied with its weight, the weighted inputs are summed, and the bias is added to it. The resulting value is the argument of the activation function. Evaluating the function gives the final result that is passed onto the next layer which performs its calculations based on the output of the previous layer. Bias and input weights are the model parameters that need to be trained given annotated input data. For example, our software extensively uses Resnet-152 (Residual Neural Network), which has a total of 115.6 million parameters<sup>27</sup>.

In image processing, two types of neural networks with different purposes are commonly used: object detection, and classification. Classification assigns an object (such as an image of a skeleton) to a predefined number of labelled classes (such as ‘supine’ or ‘flexed on left side’ to describe the pose

of the skeleton in the grave). Object detection networks, on the other hand, output a list of bounding boxes with a label for each of them. Each bounding box corresponds to a specific object detected in the image.

Models need to be trained to accurately perform the desired task. For supervised training of a model, one needs a training dataset, a loss function and an optimiser. In our case, the training dataset consists of images of objects that were manually labelled and that the algorithm learns to recapitulate. Optimisers are algorithms that are executed on the model and tweak its parameters to improve classification accuracy; or, in other words, that increase the number of times a correct label is produced for a given image. A loss function is used to quantify the prediction error, which is related to how often the model predicts incorrect labels. The output of an image classification network are the probabilities that an object belongs to each of the various labelled classes.

For classification, a widely used loss function<sup>28</sup> is cross entropy loss, defined as:

$$l(x, y) = - \sum_{c \in C} x(c) \log y(c),$$

where  $C$  is the set of classes and  $x, y$  the predicted and true probability vector, respectively. Training a model on the whole dataset once is referred to as an “epoch”. Usually models are trained for hundreds or thousands of epochs to get a satisfying result. The training data is re-shuffled randomly before every training epoch to avoid learning effects caused by a specific order.

We use two different types of models in our application, Faster R-CNN (region-based convolutional neural network)<sup>29</sup>, an object detection network here with MobileNetV3-Large 34 as its so-called backbone. We decided to use Faster R-CNN because of its performance on CPUs<sup>29</sup>, thereby enabling deployment on common server hardware – as opposed to other networks which heavily rely on the availability of GPUs. The other network that was used is Resnet (residual neural network)<sup>30</sup>. Resnet consists mostly of stacked convolutional layers, which is a common architecture for image classification networks, and represents a significant improvement over previous networks mostly as it introduced shortcut connections.

### 2.1.2 Object Detection for Graves in Legacy Sources

All the documents we used for this project were in PDF format. The uploaded documents were saved to a database and converted to separate images for each page. `Vips::Image.pdfload` is used to convert the files to single page images (ruby-vips 2.4.1 with libvips 8.9.1-2). Further pdf information such as the number of pages is obtained using `pdf-reader 2.11.0 46`. These images were then scaled and fed into an R-CNN, trained with a set of archaeological drawings.

The result is a list of bounding boxes with labels for each page. These labels include “grave”, “skeleton”, “scale” and “north arrow” among others. These bounding boxes encapsulate the relevant object as shown on the page (**figure 1**).

On their own, the objects detected in individual bounding boxes are of little use to archaeologists. Different classes of objects have to be combined to represent entities interpretable by archaeologists, and allow for metric measurements. Concretely, this means that graves have to be connected with their respective scales, north arrows, cross sections, artefacts and possible skeletons contained within the grave.

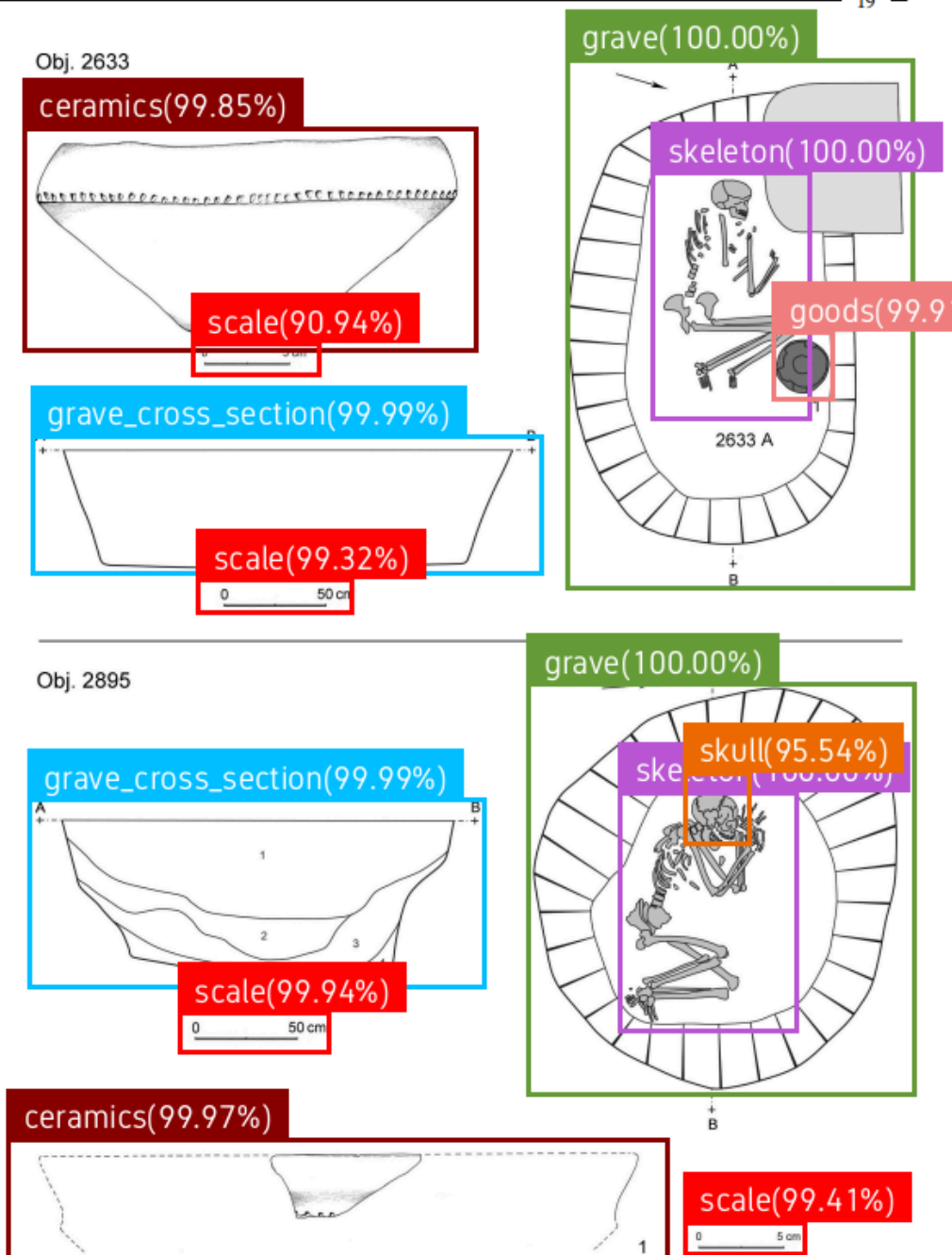
To create fully annotated graves, the algorithm first combines all graves on a page. The nearest north arrow, scale and cross-section are assigned to each grave, using the Euclidean distance measured

from the centre of the bounding boxes. These objects can be assigned to multiple graves at the same time. All skeletons and artefacts within the bounding box of the grave are then assigned to it.

Scales have to be further processed to parse the information they encode. For this, we devised a method using the contours of the bounding box detected using the OpenCV 4.6 implementation of *findContours* (based on Suzuki et al. <sup>31</sup>), and OCR (optical character recognition) with Tesseract (<https://github.com/tesseract-ocr/tesseract>). The contour analyser calculates the length of the scale while we use OCR to determine the factor for conversion from pixels into real-world distance. The text, usually a number with a length unit, from the scale is extracted and then the software tries to determine the unit of measurement (such as centimetre or metre). If a unit could be determined, the number is converted to centimetres, which the software internally uses for all measurements.

The north arrows are analysed using a Resnet-152<sup>30</sup> residual neural network that retrieves their angle. This network has been trained in an unsupervised manner as opposed to other neural networks discussed here. For every training step, those arrows are rotated by a random angle within 10° degree steps (0°, 10°, 20°, 30° ...). The rotated image is then processed by the neural network, which predicts those 10° degree bins as a label. RMSProp <sup>32</sup> (root mean square propagation) was used as the optimizer with a learning rate of 1e-3. It was trained for 1000 epochs with a batch size of 16.

We use *findContours* from OpenCV 4.6 with `RETR_EXTERNAL` and `CHAIN_APPROX_SIMPLE` to detect the outline of the burial, the north arrow, the cross section and the scale. The page image was inverted, then converted to grayscale. After this step, threshold using the OpenCV threshold method with the parameters 40 (thresh), 255 (max) and `THRESH_BINARY` (type) was performed. Then the largest contour is selected using the length of its arc. This outline is used to calculate the area, width, length and rotation of the burial. The area is retrieved using the OpenCV *contourArea* function. Width and length are created by first obtaining the bounding rectangle using *minAreaRect*<sup>33</sup>. By definition, the width is the shorter side of the rectangle, length is the longer side of the rectangle. The angle is used from the bounding rectangle as well. The poses of skeletons are classified with Resnet-152. RMSProp was used as the optimizer with a learning rate of 1e-3. It was trained 1000 epochs with a batch size of 16.



Obr. 3. Vliněves, okr. Mělník. Hroby z počátků staršího eneolitu. Půdorysy a profily podle terénní dokumentace sjednotil a překreslil M. Dobeš, nálezy nakreslila L. Jarošová, upravila B. Hružová. —Abb. 3. Vliněves, Kreis Mělník. Gräber vom Anfang des älteren Äneolithikums.

**Figure 1.** Example of the object detection result for one page of catalogue (here: Corded Ware site of Vliněves<sup>1</sup>, Czech Republic). Results for North arrows were excluded for better visibility.

We identified several challenging constellations when using the aforementioned method on a wide variety of publications. Occasionally, objects are incorrectly assigned to a grave based on the distance. Often this is because multiple scales are present on the page and the nearest scale belongs to an artefact instead of a grave. False negatives can also occur, leading other objects to be incorrectly grouped with a grave, such as north arrows belonging to a different drawing on the same page.



A list of all graves in a publication is automatically generated once the process is complete. Each entry must subsequently be manually validated.

## 2.2 Datasets

The primary dataset is the one for detecting graves and objects therein. Two derived datasets are also considered – they deal with skeleton pose and arrow-type classification for skeletons and arrows detected via the primary dataset.

### 2.2.1 Object Detection Training Dataset

As a primary dataset, we used catalogues of 3<sup>rd</sup> millennium BCE graves, which we manually annotated for object detection using *labelImg* (<https://github.com/HumanSignal/labelImg>). In total, 391 pages were annotated (**table 1**). The quality and detail of the annotated material range from high-resolution digital catalogues, such as those published for the sites of Vliněves in the Czech Republic <sup>1,34</sup>, to lower-quality book scans and even hand-drawn notes from Southeast European and Russian excavations. The corresponding archaeological sites are shown in **figure 2**.

Each page of these documents was converted to an image and randomly sampled. At first we annotated all pages with drawings from four publications for our initial proof of concept <sup>1,34-36</sup>. For the extended dataset a random sample was used and a manual selection was done to maximise the number of pages containing relevant drawings.

Class label	Object count	Scanned hand-drawn images	Scanned digital images	Digital illustrations
grave	376	72	82	222
text	850	174	116	560
skeleton photo	52	6	0	46
ceramics	615	132	128	355
artefact	535	342	99	94
grave photo	122	4	2	116
map	59	9	11	39
scale	905	236	155	514
arrow	532	160	118	254
skeleton	404	146	91	167
grave artefact	207	8	26	173
grave cross section	240	44	19	177

stone tool	346	112	180	54
shaft axe	121	2	111	8

**Table 1.** Number of annotated objects in the primary dataset per class and image quality (see supplementary material for list).

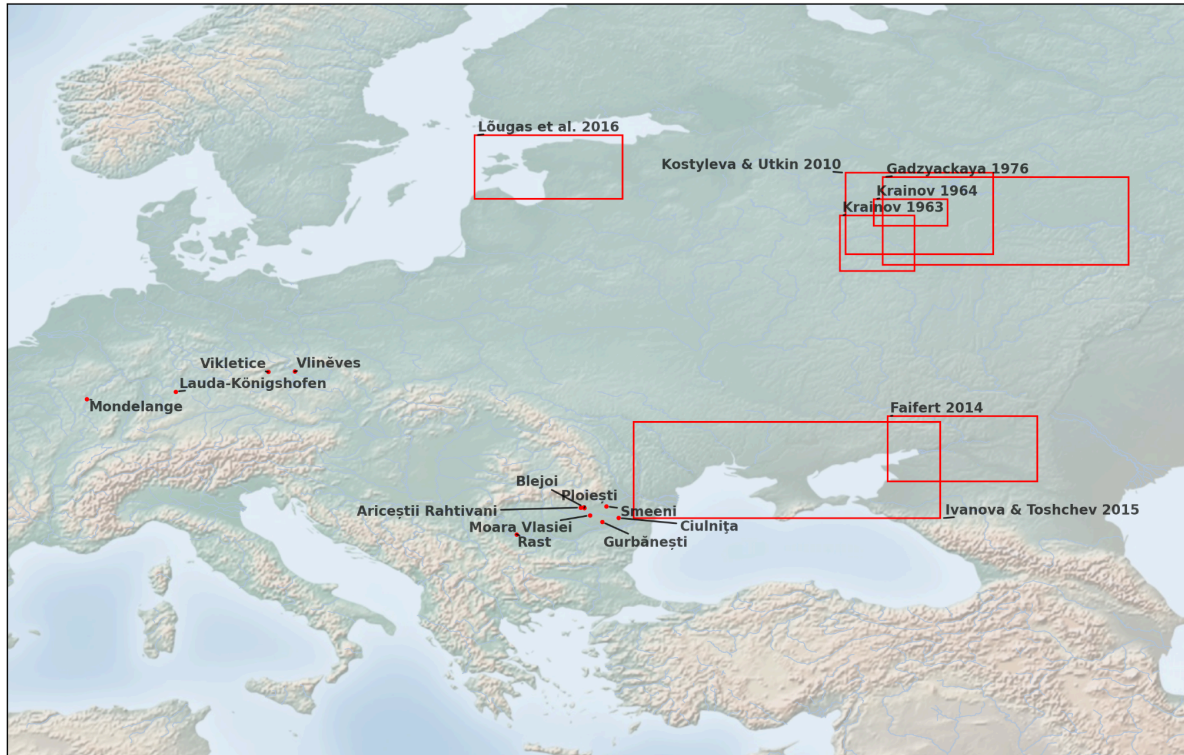


**Figure 2.** Map of sites used in training and/or validation (drawn with Matplotlib Basemap Toolkit 1.3.8 and Python 3.11; background is a display shaded relief image from <http://www.shadedrelief.com>).

### 2.2.2 Skeleton Pose Classification Dataset

From the object detection training dataset all skeleton images were extracted using their labelled bounding box. These images were manually assigned to two classes, “supine” and “flexed on the side”. All images that could not be clearly distinguished were removed. This led to 239 drawings of skeletons in supine position and 133 of skeletons flexed on one side being collected. They were all resized to 300x300 pixels to provide a uniform resolution.

### 2.2.3 Arrow Classification Dataset

All north arrows were extracted from the object detection training dataset. Then a manual selection was performed to have an even spread of different types of arrows. In total, we chose 118 north arrows. These were scaled to 224x224 pixels and rotated to point towards 0° degrees.

## 3 The AI-assisted Workflow

### 3.1 Workflow Steps

The full semi-automated workflow for annotation consists of six distinct steps – with appropriate support by the graphical user interface of the *AutArch* software:

*Step 1. Basic grave information.* The ID assigned to the burial by the authors in the source publication is recorded. In case multiple images of the same grave are shown, the software will prevent duplicates in the results using this ID. In this step, the expert also has the option to discard drawings incorrectly classified as a grave.

*Step 2. Correcting bounding boxes.* The user can manually add, remove or change the bounding box assigned to a specific grave. Potential tasks include selecting a different scale on the page, resizing bounding boxes because they do not fully encapsulate an object or marking north arrows that were initially missed by object detection. During this step, a manual arrow has to be drawn for every skeleton following the spine and pointing towards the skull, which is necessary to determine the exact orientation of the skeleton in the grave. With the completion of this step several automated steps are performed. The contours are calculated using the new bounding boxes and the resulting changes in measurements are saved. The orientation of the north arrow and the deposition type of the skeleton are updated using their respective neural network. The analysis of the scale is performed again. In case an arrow through the spine of the skeleton was added, the angle is calculated as follows:  $f(a_x, a_y, a_\alpha, s) = \text{atan}^2(a_x, a_y) - \text{atan}^2(-\sin(a_\alpha)) - \cos(-a_\alpha)$ , with positive angles  $a$  ( $a = a' + 360^\circ$  if  $a' < 0^\circ$ ) mapped to the interval  $[0, 1]$  by the transformation  $a \frac{180}{\pi}$ , where  $a_x$  and  $a_y$  are the x and y coordinate of the vector of the spine orientation arrow.

*Step 3. Contour validation.* All detected outlines in relation to one particular grave are highlighted, allowing the user, if any issue arises, to return to the previous step and fit, for instance, a manual bounding box around the grave or cross-section to indicate the width, length or depth.

*Step 4. Scale information.* The next step is to validate the scale. The text indicating the real-world length of the scale has to be checked. Once this step is completed, all measurements are updated with the new scale information. In case no individual scale is provided and the publication uses a fixed scale, e.g. all drawings are 1:20, a different screen is shown. In this screen, the actual height of the page (in cm) has to be entered manually, together with the scale of the drawing. This way, all measurements can be calculated in the absence of a scale and the results are fully compatible with scaled publications.

*Step 5. North arrow orientation.* The angle of the north arrow can be adjusted manually based on a preview. In case an arrow is missing in the drawing, this screen will be skipped and size measurements and contours will still be collected without the orientation. In some cases, there were no north arrows in the drawing to indicate the orientation of the drawn feature.

*Step 6. Skeleton pose.* Finally, the pose of all skeletons has to be validated, which (for now) consists of “unknown”, “flexed on the side” or “supine”. As described above, a neural network will set the initial body position, but it can be adjusted manually. Further positions could easily be added in the future. “Unknown” is used in cases where skeletal remains are visible, but no position can be identified.

## 3.2 Manual Validation and Adjustment

The workflow is supported by a graphical user interface (as part of the *AutArch* software) that allows manual correction of the annotations obtained through the automated process described above. Although our automatic approach is accurate for most publications, validation and potential manual correction by a domain expert are essential to maximise the reliability of the archaeological annotations. The graphical interface is a web application that is usable on a wide variety of devices including mobile devices. While we currently focus on drawings of graves, other types of objects such as ceramics could be analysed with minor modifications.

Our two-part workflow uses an automated process and a manual process. Because a core feature is the marking of objects with their bounding boxes, it differs from other software-supported workflows commonly used to analyse drawings with CAD or image processing applications. In **figure 3**, we illustrate manual adjustment, as supported by the *AutArch* graphical user interface.

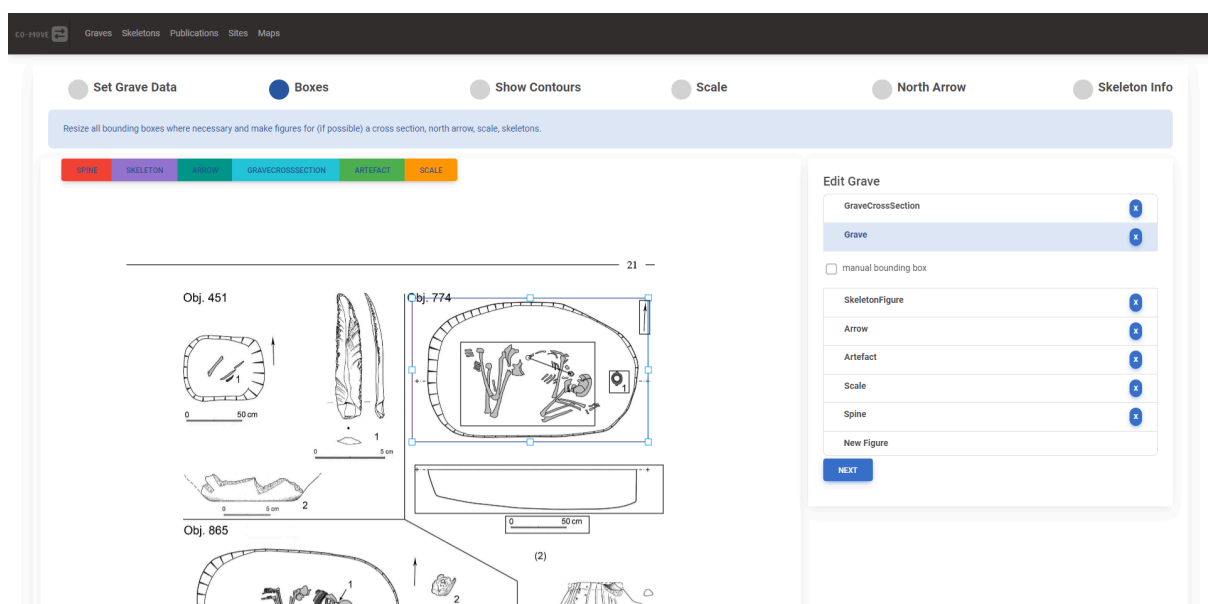


**Figure 3.** Screenshot of the manual validation process; note the resizing of the box around the grave.

## 3.3 Data Analytics and Visualisation

On top of the step-by-step workflow, the *AutArch* software also supports data analytics and visualisation of summary data for multiple graves or publications in terms of the orientation of skeletons or the geometry of whole-outlines. Our method of aggregating archaeological data is tailored towards supporting the creation of uniform assemblages.

Publications are visualised as a whole with a variety of charts. Several publications can be compared in the software. In this case, the data is usually presented in the same chart and is assigned a specific colour that is consistent through different visualisations. All data points are linked to their respective burials and can be navigated.

### 3.3.1 Orientation of Skeletons

The orientations of burials are shown using radial charts. Two types of orientations can be used (**figure 4**): a) *skeletons* within burials that have a discernible body position; or b) (**figure 5**) the orientation of the long side of the bounding box encapsulating the object. The outline orientation is given between 0 and 180 degrees, because the bounding box *per se* lacks direction.

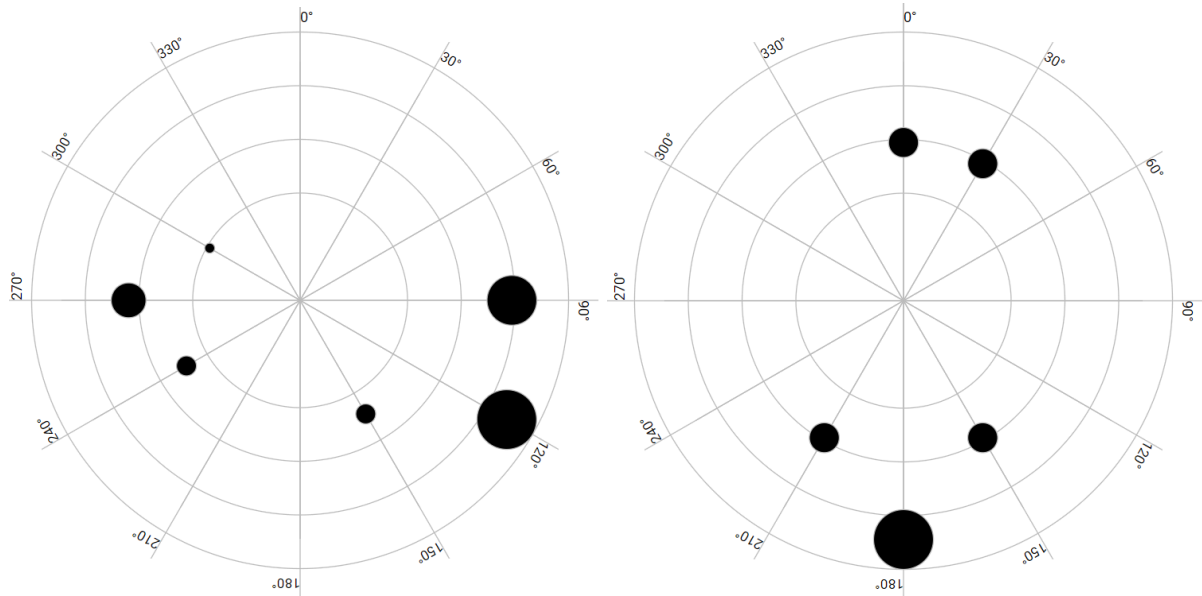


**Figure 4.** An example of numerical attribute that can be automatically retrieved using the AI-assisted workflow: the orientation of ‘Corded Ware’<sup>1</sup> (left, n = 39) and ‘Bell Beaker’<sup>34</sup> (right, n = 6) graves with skeletons from the site of Vliněves, Czech Republic.

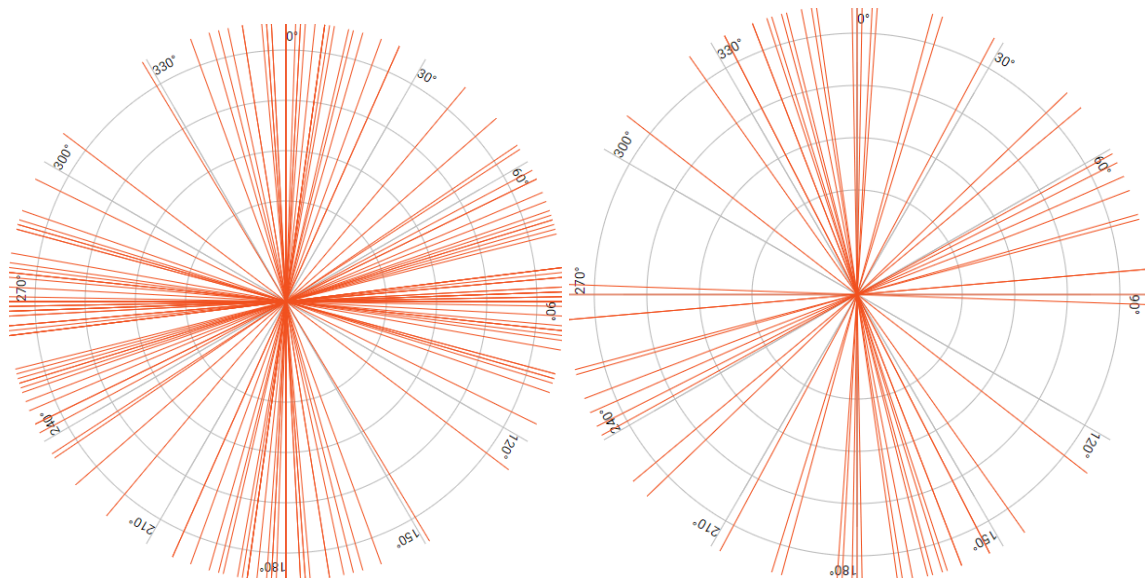


**Figure 5.** Orientation of the long side of the bounding box encapsulating graves of ‘Corded Ware’<sup>1</sup> (left, n = 87) and ‘Bell Beaker’<sup>34</sup> (right, n=33) from the site of Vliněves, Czech Republic.

We analysed four different publications<sup>1,4,34,37</sup>, including two that were previously used for manual validation as a proof-of-concept. Those are part of the object detection training set. A further two publications were analysed.

*AutArch* performs descriptive statistical analysis for data visualisation purposes. We compared the burials from Vliněves, which were attributed to the ‘Corded Ware’ (Dobes & Limburský 2013) culture with those attributed to the ‘Bell Beaker’ (Limburský 2012). Our data, as visualised in **figure 4**, shows differences (albeit non-significant, Watson’s  $U^2$  test  $p=0.15$ ) in the orientation of the skeletons between the two.

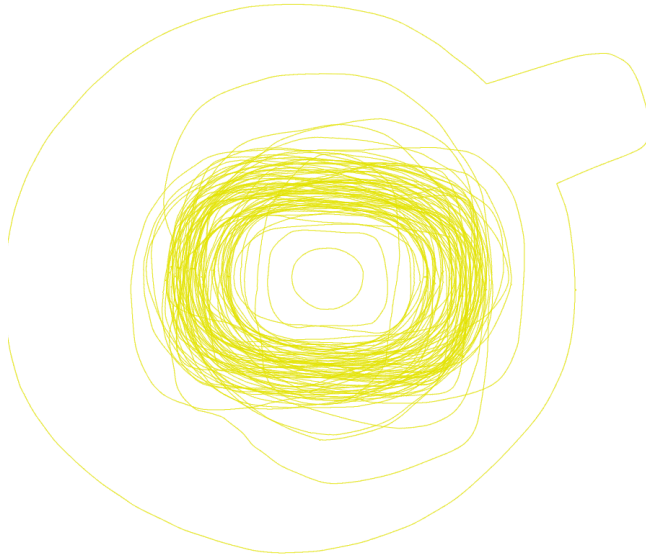
### 3.3.2 Basic Geometry of Whole-outlines of Graves

Outlines of graves can be overlaid to visualise their shape (**figure 6**). These outlines are corrected in size through the scales in the drawing or a fixed one and the orientation is normalised using the given arrows. Even though the full outlines of burial pits are an intermediate step to calculate their outside measurements, they also represent interesting data in themselves. The figure shows the geometric whole-outlines of graves from their respective publications stacked over each other. Drawings that have no automatically detectable outline and use the manual bounding box instead are excluded here.

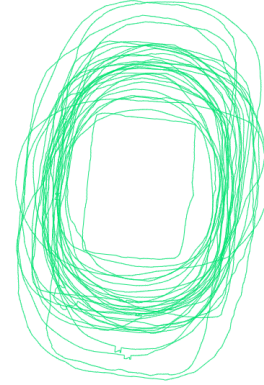
### 3.3.3 PCA for comparison of Whole-outlines of Graves

The sizes of burial pits are charted by converting the width, depth, length and bounding box orientation to two dimensions using EFD and PCA. That is, *AutArch* can visualise grave outlines by transforming them and then projecting the resulting data on a scatter chart (**figure 7**). We applied the methodology described in Matzig et al. 2021<sup>18</sup> and modelled the outlines by EFDs (elliptic fourier descriptors) with 15 harmonics, projected on two dimensions with PCA (principal component analysis). Besides several outliers, the outlines of pit graves belonging to both ‘Corded Ware’ and ‘Bell Beaker’ were too similar to distinguish reasonable groups, underscoring their close cultural affinity<sup>38</sup>.

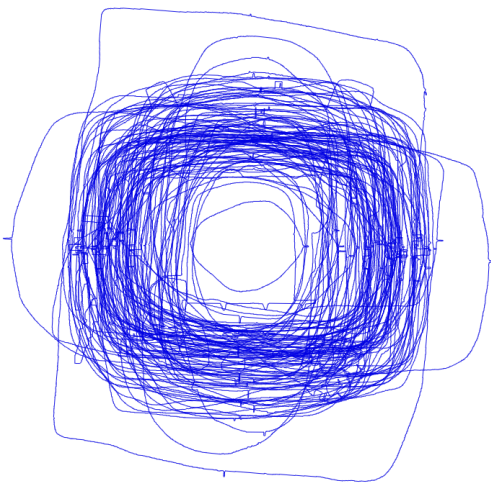
Vliněves 'Corded Ware' (n = 78)  
Dobeš and Limburský 2013



Vliněves 'Bell Beaker' (n = 31)  
Limburský 2012



Vikletice 'Corded Ware' (n = 102)  
Buchvaldek & Koutecký 1970



Mondelange 'Bell Beaker' (n = 19)  
Gazenbeek et al. 2009



**Figure 6.** Shape variation (geometric 'whole-outlines'). Here grave outlines or cuts, retrieved through contour detection from four publications <sup>1,4,34,37</sup>, were automatically scaled and rotated using the AI-assisted workflow.

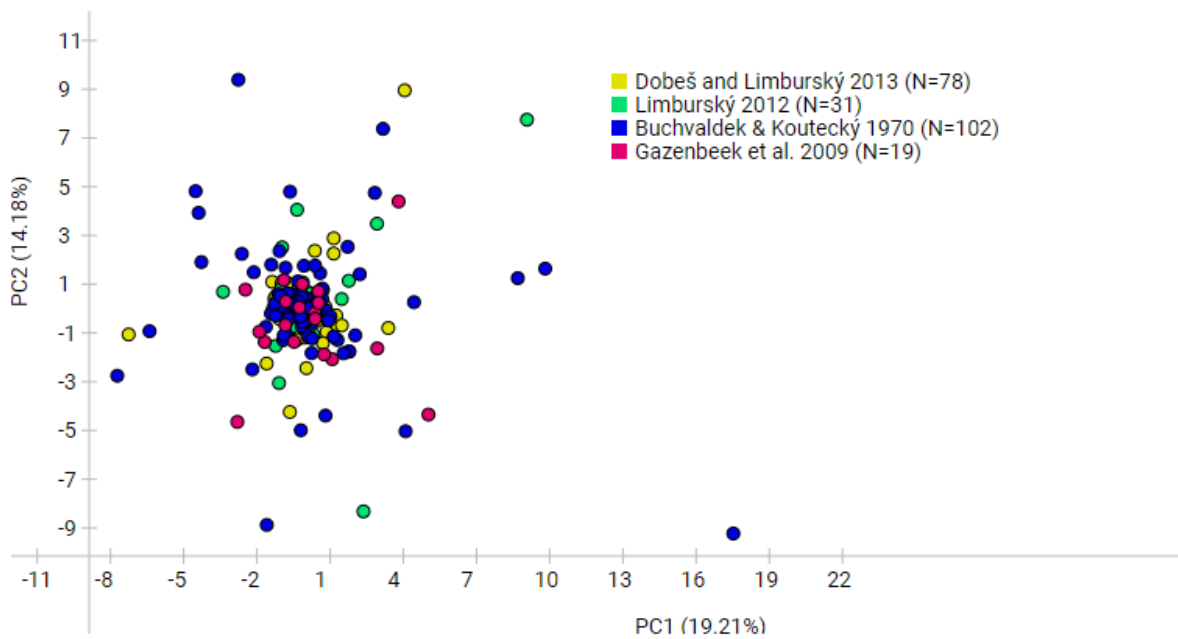


**Figure 7.** Geometric whole-outlines of graves using EFD (15 harmonics) projected on the first two principal components.

## 4 Results

The main results of the reported research are:

- most importantly, a workflow for data collection,
- relying on an approach to object detection tailored to the archaeological scope at hand,
- using a labelled dataset (**table 1**) of catalogues of 3rd millennium BCE graves,
- training a model,
- analysing the data obtained from selected publications <sup>1,4,34,37</sup> and others.

In this section, we discuss evaluation of object detection, workflow, and the achievable user experience. The data related to this evaluation is published as part of the *online resources*, as discussed in the introduction of the paper.

### 4.1 Evaluation of Object Detection by Metrics

To evaluate the software's ability to detect graves in archaeological publications, we performed a qualitative analysis on publications, which cover both related and different archaeological periods compared to our training dataset, including European Early Neolithic, Chalcolithic and Early Bronze Age graves.

Publication	true positive	false positive	false negative
Włodarczak 2018 <sup>39</sup>	13	0	0



Baron et al. 2019 <sup>40</sup>	2	0	0
Sachsse 2015 <sup>41</sup>	53	2	12
Neugebauer-Maresch and Lenneis 2015 <sup>42</sup>	84	22	4

**Table 2.** Object detection results for graves in different publications.

As **table 2** illustrates, object detection performed perfectly for two of the four publications, whereas there were false positives and negatives (i.e., incorrectly detected or missed graves) affecting approximately 1/4 of the total number of graves to be detected for the two remaining publications. It is worth noting that the current training dataset of just 391 is rather small when compared to other commonly used datasets such as COCO 40. Additional training is bound to improve the object detection rate.

## 4.2 Evaluation of Workflow by Metrics

As an estimation of the necessary manual work that is needed, we tracked all necessary changes that needed to be performed for Włodarczak 2018 <sup>39</sup> (also mentioned in **table 2**). Only steps that could have been correctly performed by the automated step have been recorded, manually adding an arrow indicating the skeletal orientation or entering the unique ID of a burial is not included. All graves were correctly detected in Włodarczak 2017, so no manual marking of burials was necessary in a separate previous step.

Grave	AS	AA	ST	AF	MB	DT	GB	AMS	AAD	Sum
III/3	●	●	●	●						4
3A/7	●	●			●	●				4
2/2	●	●		●		●	●			5
6/24		●	●					●		3
7/14		●	●	●			●			4
5		●	●	●		●		●		5
2/5					●					1
1B					●					1
1/5			●			●			●	3
3/2			●	●		●	●	●		5
6/2				●	●	●				3
8/2				●			●			2
5/1				●	●					2
<b>Sum</b>	<b>3</b>	<b>6</b>	<b>6</b>	<b>8</b>	<b>5</b>	<b>6</b>	<b>4</b>	<b>3</b>	<b>1</b>	

**Table 3.** Necessary manual corrections for Włodarczak 2018 <sup>39</sup>. Abbreviations: AS = adjusted scale, AA = added north arrow, ST = text entered for a scale, AF = north arrow flipped by 180°, MB = manual bounding box, DT = entered deposition type, GB = resized grave bounding box, AMS = added missing skeleton, AAD = arrow adjusted.

As **table 3** illustrates, the automation of the different workflow steps fails at times and manual assistance is required. For the sample at hand, approximately three manual corrections are required per grave on average. Still the guided workflow and the tool support for performing such manual adjustments further contribute to productivity and consistency.

### 4.3 Evaluation by User Study

To evaluate the correctness and potential productivity benefits of the software and the workflow, we invited 10 participants to perform small computing tasks for 90 minutes at the Anthropological Institute of Johannes Gutenberg University Mainz. The test group consisted of undergraduate students, postgraduate and postdoctoral researchers from a variety of backgrounds, including archaeologists and non-archaeologists.

The participants had no prior experience with the AI software presented in this manuscript. We also made sure that none of the participants were able to read Czech, because we wanted to prevent the participants from reading the textual descriptions instead of analysing the drawings<sup>1</sup>.

An earlier version of our AI software, *AutArch*, however with the same AI models, was used in the user study. Based on the feedback and insight gathered during the study, we later made improvements to the software and to the graphical user interface.

Participants were divided into two groups. The first group began with *Inkscape* and then moved on to *AutArch*, while the second group began with *AutArch* and then moved to *Inkscape* – with these two phases being timed and limited to 30 minutes. This is an AB/BA study format, as common in controlled experiments.

The two groups were given a very short induction to *Inkscape*. They were asked to import PDF pages containing graves from Dobeš and Limburský 2013<sup>1</sup> into *Inkscape*, then manually measure each grave using the measuring function. A standard excel spreadsheet was provided with formulas to work out the actual size of graves based on the scale. We also gave a short introduction on how to use *AutArch*. Participants were asked to record the grave ID, make necessary corrections to the bounding boxes, draw arrows through the spines and validate the scales, arrows and the deposition type. This publication<sup>1</sup> had already been imported into *AutArch*. We decided to have the participants import the PDF into *Inkscape* as opposed to it being imported already, because importing the whole PDF into *Inkscape* led to a significant performance reduction of the software. Participants were provided with a checklist for a number of steps – the current version of the software provides a more guided workflow instead of a checklist.

The results of the experiment are shown in **figure 8**. Manually collected data and the participants' *AutArch* results, i.e. width, length etc., were compared to a baseline that we created using *AutArch* ourselves and the percentage deviation was recorded. The deviation of all values for a single grave was summed up and the average error was calculated between all graves for both *Inkscape* and *AutArch*. In instances where values were missing, these specific values were skipped in the error calculation. Situations where certain values could not be obtained such as with missing cross-sections were omitted. We observed that the use of our AI-software (*AutArch*) resulted in considerably fewer errors (in % of the baseline) and was faster than manual recording using *Inkscape* (number of graves for each participant in a 30-minute window).

Despite the relatively low number of participants, the user study successfully demonstrates that our AI-assisted workflow performs significantly better than manual measurement using a drawing software, i.e., it is significantly faster and less prone to errors (**figure 8**). Two of the participants exhibited larger errors than the other participants. We assume that different experience levels in

working with computers affect the performance of our software at the same level as alternatives. We expect this effect to become more pronounced the longer these tasks are performed, due to the onset of mental fatigue.

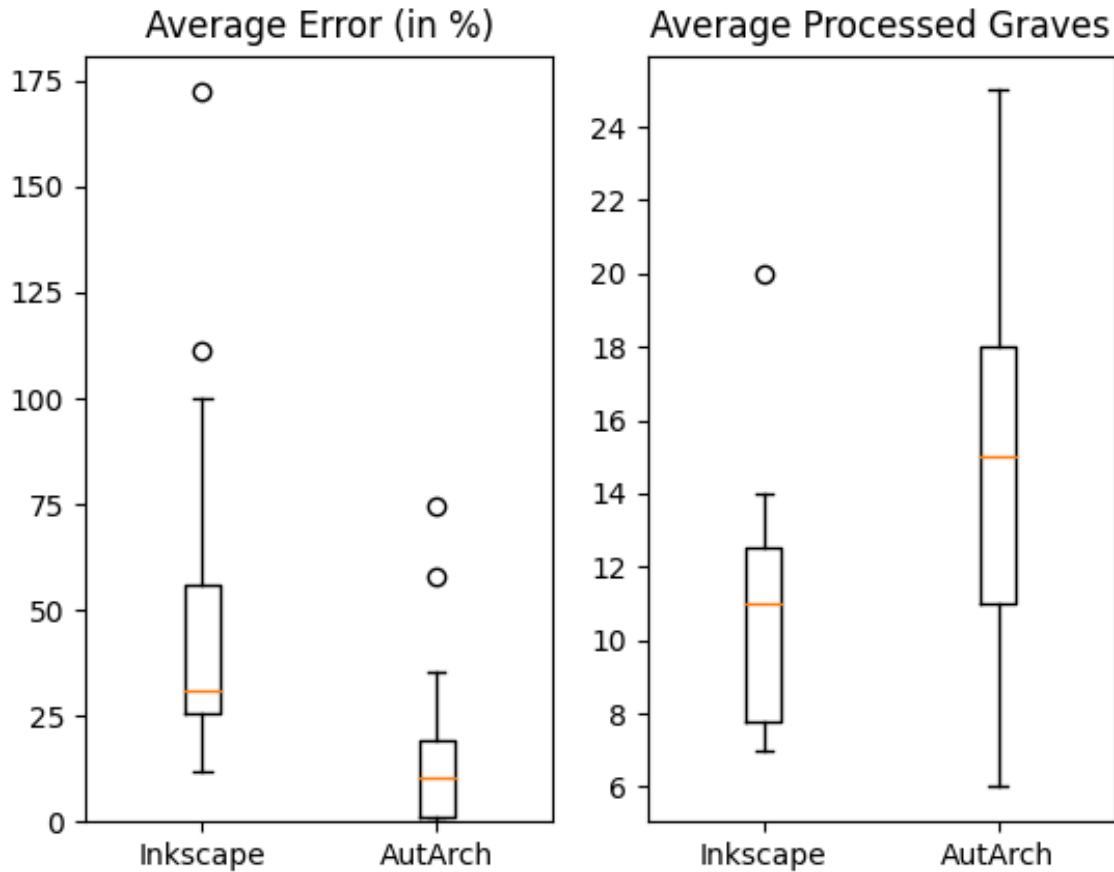


*Figure 8. Results of the user study.*

## 5 Conclusions

### Summary

In this paper, we have presented a new AI-supported workflow to tackle the challenge of large-scale archaeological data collection. Our approach improves speed and accuracy of manual methods, as demonstrated by the user study. The workflow benefits arise as a result of the use of AI-based object detection and more generally image processing as well as the use of a software-based approach (*AutArch*) towards workflow management in the relevant archaeology domain. Also, our shape-related measurements of width, length and depth of burial pits are collected in a standardised manner. This allows to perform meta-analyses across different publications and to define and detect outliers with unusual shapes. Our approach also increases the precision of measured angles to assess the orientation of skeletons and burial pits. Furthermore, the automated detection of contours combined with EFD offers an alternative to landmark-based geometric morphometrics<sup>18</sup>.

The collection of material for this kind of analysis has been a time-consuming task in the past, forcing researchers to normalise basic parameters such as size <sup>18</sup>, because scaling every single object was not practical. With our approach, we can harmonise the scales of every object to allow for meaningful comparisons. The emerging database will allow for complex, composite queries over all recorded attributes, such as burials within specific dimensions, with specific orientations and/or with a certain number of skeletons.

## Future Work

There is huge potential to improve data collection in archaeology for other objects beside graves, including but not limited to buildings, ceramics, stone tools and arrowheads. Recording these objects is not limited to academic research, but it could also be used for commercial archaeology and cultural heritage. Even large amounts of unpublished hand drawings could be analysed and integrated into a database. A new standard for documenting archaeological features for graves and such might need to be created to ease integrations with software that can automatically digitise handwritten documentation and provide a general improvement in standardisation.

Applying our method to other aspects of material culture, for instance, ceramic ware, would require a broader set of attributes. These would include the fabric and surface treatment among many other attributes. Published text might contain further information, but its analysis will be a future task. Analysing the text of publications using established statistical NLP (natural language processing) or incorporating text into image classification using multi modal AI <sup>43</sup> provide opportunities for more efficient and extensive data collection. This could also improve the current aspects of the workflow. For example by combining textual information about burial measurements, the plausibility of the assignment of specific arrows or scales to burials could be checked.

Our software uses well established high performance neural networks that work well with most existing and even older hardware. There have been significant advances in two areas of machine learning: more performant hardware and better performing networks <sup>44</sup>. TPUs (tensor processing units) offer a significant improvement over conventional CPUs or GPUs for machine learning use cases. Newer network architectures, such as Vision Transformers <sup>45-47</sup> have greatly increased performance, compared to Resnet-152 or Faster R-CNN used in our application.

An ethical risk of introducing *AutArch* to a wider audience is the potential automation of repetitive jobs by AI such as database entry and curation, typically performed by paid trainees and technicians. This risk is present in all sectors where AI is being deployed. *AutArch* requires a human agent to manually validate database entries. In theory, the AI-assisted workflow should make the recording process significantly less tedious, freeing up time for more creative tasks like literature search and data analysis.

## Author Contributions

Conceptualization: K.K., M.B. Data curation: K.K., A.V.G. Formal analysis: K.K. Funding acquisition: M.B. Investigation: K.K., M.B., A.V.G. Methodology: K.K., A.W. Project administration: M.B. Resources: K.K., M.B., A.V.G. Software: K.K. Supervision: M.B. Validation: K.K., M.B., Y.D., V.H. R.L. Visualisation: K.K. Writing – original draft: K.K., M.B. Writing – review & editing: K.K., A.V.G., A.W., R.L., Y.D., M.B. All authors reviewed the manuscript.

## Acknowledgements

We thank Bianca Preda-Bălănică and Stefano Palalidis for their help with ‘Yamnaya’ references. We are also grateful to Miroslav Dobeš and Petr Limburský for the permission to reproduce illustrations from Vliněves. This research was supported by the German Science Foundation (DFG Project CO-MOVE, Grant n° 466680522, awarded to Maxime Brami). Volker Heyd's and Yoan Diekmann's contributions to this study were supported by the European Research Council (ERC) under the European Union's Horizon 2020 research and innovation program (Grant agreement n° 788616-YMPACT).

## Training Dataset

Bader 1963 <sup>48</sup>, Bader & Khalikov 1976 <sup>49</sup>, Buchvaldek and Koutecký 1970 <sup>37</sup>, Comsa 1989 <sup>50</sup>, Dobeš & Limburský 2013 <sup>1</sup>, Dumitrescu 1980 <sup>51</sup>, Frînculeasa 2013 <sup>52</sup>, Frînculeasa et al. 2015 <sup>21</sup>, Frînculeasa et al. 2017 <sup>53</sup>, Frînculeasa et al. 2018 <sup>54</sup>, Frînculeasa 2019 <sup>55</sup>, Frînculeasa 2020 <sup>56</sup>, Frînculeasa et al. 2021 <sup>57</sup>, Frînculeasa et al. 2022 <sup>58</sup>, Gadzyackaya 1976 <sup>59</sup>, Gymashian 1993 <sup>60</sup>, Ivanova & Toshchev 2015 and references therein <sup>61</sup>, Kostyleva & Utkin 2010 <sup>62</sup>, Krainov 1963 <sup>63</sup>, Krainov 1964 <sup>64</sup>, Langova 2009 <sup>35</sup>, Limburský 2012 <sup>34</sup>, Lougas et al. 2007 <sup>65</sup>, Papac et al. 2021 <sup>66</sup>, Rosetti 1959 <sup>67</sup>, Toshchev, Shapovalov, Mikhailov 1991 and references therein <sup>68</sup>.

## References

1. Dobeš, M. & Limburský, P. *Pohřebiště staršího eneolitu a šňůrové keramiky ve Vliněvsi*. vol. 22 (Vydal Archeologický ústav AV ČR, 2013).
2. Kristiansen, K. Towards a new paradigm? The third science revolution and its possible consequences in archaeology. *Curr. Swed. Archaeol.* **22**, 11–34 (2014).
3. Museum of London Archaeology Service. *Archaeological Site Manual*. (Museum of London, 1994).
4. Gazenbeek, M. *et al.* *Mondelange (57, Moselle), 'PAC de la Sente', volume I: textes (Rapport final d'opération)*. (INRAP, 2009).
5. Ortolf, S. E. Das schnurkeramische Gräberfeld von Lauda-Königshofen im Taubertal. *Fundberichte Aus Baden-württemberg* **34**, 410–528 (2014).
6. Wentink, K. *Stereotype: The role of grave sets in corded ware and bell beaker funerary practices*. (Sidestone Press, 2020).
7. Gansell, A. R., Meent, J.-W. van de, Zairis, S. & Wiggins, C. H. Stylistic clusters and the Syrian/South Syrian tradition of first-millennium BCE Levantine ivory carving: a machine learning approach. *J. Archaeol. Sci.* **44**, 194–205 (2014).
8. Grosman, L., Karasik, A., Harush, O. & Smilanksy, U. Archaeology in three dimensions: Computer-based methods in archaeological research. *J. East. Mediterr. Archaeol. Herit. Stud.* **2**, 48–64 (2014).
9. Hörr, C., Lindinger, E. & Brunnett, G. Machine learning based typology development in archaeology. *J. Comput. Cult. Herit.* **7**, 1–23 (2014).
10. Pawłowicz, L. M. & Downum, C. E. Applications of deep learning to decorated ceramic typology and classification: A case study using Tusayan White Ware from Northeast Arizona. *J. Archaeol. Sci.* **130**, 105375 (2021).
11. Berganzo-Besga, I., Orengo, H. A., Lumbreras, F., Aliende, P. & Ramsey, M. N. Automated detection and classification of multi-cell Phytoliths using Deep Learning-Based Algorithms. *J. Archaeol. Sci.* **148**, 105654 (2022).
12. Klassen, S., Weed, J. & Evans, D. Semi-supervised machine learning approaches for predicting the chronology of archaeological sites: A case study of temples from medieval Angkor, Cambodia. *PLoS One* **13**, e0205649 (2018).
13. Guyot, A., Hubert-Moy, L. & Lorho, T. Detecting Neolithic Burial Mounds from LiDAR-Derived Elevation Data Using a Multi-Scale Approach and Machine Learning Techniques. *Remote Sensing* **10**, 225 (2018).
14. Lambers, K., Verschoof-van der Vaart, W. B. & Bourgeois, Q. P. J. Integrating Remote Sensing, Machine Learning, and Citizen Science in Dutch Archaeological Prospection. *Remote Sensing* **11**, 794 (2019).
15. Wernke, S., VanValkenburgh, P. & Saito, A. Interregional Archaeology in the Age of Big Data: Building Online Collaborative Platforms for Virtual Survey in the Andes. *J. Field Archaeol.* **45**, S61–S74 (2020).
16. Lane Fox, A. H. On a Series of About Two Hundred Flint and Chert Arrowheads, Flakes, Thumbflints, and Borers, from the Rio Negro, Patagonia; with Some Remarks on the Stability of Form Observable in Stone Implements. *The Journal of the Anthropological Institute of Great Britain and Ireland* **4**, 311–323 (1875).
17. Resler, A., Yeshurun, R., Natalio, F. & Giryes, R. A deep-learning model for predictive archaeology and archaeological community detection. *Humanities and Social Sciences Communications* **8**, 1–10 (2021).

18. Matzig, D. N., Hussain, S. T. & Riede, F. Design Space Constraints and the Cultural Taxonomy of European Final Palaeolithic Large Tanged Points: A Comparison of Typological, Landmark-Based and Whole-Outline Geometric Morphometric Approaches. *Journal of Paleolithic Archaeology* **4**, 27 (2021).
19. Araujo, R. P. *et al.* Benchmarking methods and data for the whole-outline geometric morphometric analysis of lithic tools. *Evol. Anthropol.* **32**, 124–127 (2023).
20. Vander Linden, M. Le phénomène campaniforme dans l'Europe du 3ème millénaire avant notre ère: synthèse et nouvelles perspectives. (2006).
21. Frînculeasa, A., Preda, B. & Heyd, V. Pit-Graves, Yamnaya and Kurgans along the Lower Danube: Disentangling IVth and IIIrd Millennium BC Burial Customs, Equipment and Chronology. *Praehistorische Zeitschrift* **90**, 45–113 (2015).
22. Kaiser, E. & Winger, K. Pit graves in Bulgaria and the Yamnaya Culture. *Praehistorische Zeitschrift* **90**, 114–140 (2015).
23. Furholt, M. Upending a 'Totality': Re-evaluating Corded Ware Variability in Late Neolithic Europe. *Proceedings of the Prehistoric Society* **80**, 67–86 (2014).
24. Nicolis, F. *Bell Beakers Today: Pottery, People, Culture, Symbols in Prehistoric Europe: Proceedings of the International Colloquium Riva Del Garda (Trento, Italy) 11-16 May 1998*. vol. 1 (Provincia autonoma di Trento, Servizio beni culturali, Ufficio beni archeologici, 2001).
25. Vander Linden, M. What linked the Bell Beakers in third millennium BC Europe? *Antiquity* **81**, 343–352 (2007).
26. Beckerman, S. M. *Corded ware coastal communities*. (Sidestone Press, 2015).
27. Leong, M. C., Prasad, D. K., Lee, Y. T. & Lin, F. Semi-CNN Architecture for Effective Spatio-Temporal Learning in Action Recognition. *NATO Adv. Sci. Inst. Ser. E Appl. Sci.* **10**, 557 (2020).
28. Mao, A., Mohri, M. & Zhong, Y. Cross-Entropy Loss Functions: Theoretical Analysis and Applications. *arXiv [cs.LG]* (2023).
29. Ren, S., He, K., Girshick, R. & Sun, J. Faster R-CNN: Towards Real-Time Object Detection with Region Proposal Networks. *IEEE Trans. Pattern Anal. Mach. Intell.* **39**, 1137–1149 (2017).
30. He, K., Zhang, X., Ren, S. & Sun, J. Deep residual learning for image recognition. *and pattern recognition* (2016).
31. Suzuki, S. & Be, K. Topological structural analysis of digitized binary images by border following. *Computer Vision, Graphics, and Image Processing* **30**, 32–46 (1985).
32. Hinton, G., Srivastava, N. & Swersky, K. Neural Networks for Machine Learning. Preprint at [https://www.cs.toronto.edu/~tijmen/csc321/slides/lecture\\_slides\\_lec6.pdf](https://www.cs.toronto.edu/~tijmen/csc321/slides/lecture_slides_lec6.pdf).
33. Structural Analysis and Shape Descriptors. Preprint at [https://docs.opencv.org/4.x/d3/dc0/group\\_\\_imgproc\\_\\_shape.html#ga3d476a3417130ae5154aea421ca7ead9](https://docs.opencv.org/4.x/d3/dc0/group__imgproc__shape.html#ga3d476a3417130ae5154aea421ca7ead9).
34. Limburský, P. *Pohřebišťe kultury se zvoncovitými poháry ve Vliněvsi : k problematice a chronologii konce eneolitu a počátku doby bronzové*. vol. 12 (Filozofická fakulta Univerzity Karlovy v Praze, 2012).
35. Langová, M. Výpověď objektů s lidskými kosterními pozůstatky na sídlišti únětické kultury ve Vliněvsi, okr. Mělník. (Univerzita Karlova, 2009).
36. Dobeš, M., Limburský, P. & Kyselý, R. Příspěvek k prostorovému uspořádání obytných areálů z konce středního eneolitu Rivnáčské osídlení ve Vlněvsi. *Archeologické* (2011).
37. Buchvaldek, M. & Koutecký, D. *Vikletice: ein schnurkeramisches Gräberfeld*. vol. III (Universita Karlova, 1970).
38. Furholt, M. Social Worlds and Communities of Practice: a polythetic culture model for 3rd

- millennium BC Europe in the light of current migration debates. *Préhistoires méditerr.* (2020) doi:10.4000/pm.2383.
39. Włodarczak, P. Kurgan rites in the Eneolithic and Early Bronze Age Podolia in light of materials from the funerary ceremonial centre at Yampil. *Balt.-Pontic Stud.* **22**, 246–283 (2018).
  40. Baron, J., Furmanek, M., Hałuszko, A. & Kufel-Diakowska, B. Differentiation of burial practices in the Corded Ware Culture. The example of the Magnice site in SW Poland. *Praehistorische Zeitschrift* **93**, 169–184 (2019).
  41. Sachße, C. *Untersuchungen zu den Bestattungssitten der Badener Kultur*. vol. 179 (Verlag Dr. Rudolf Habelt, 2010).
  42. Neugebauer-Maresch, C. & Lenneis, E. *Das linearbandkeramische Gräberfeld von Kleinhadersdorf*. (Verlag der Österreichischen Akademie der Wissenschaften, 2015).
  43. Singh, A. *et al.* FLAVA: A foundational language and vision alignment model. *arXiv [cs.CV]* 15638–15650 (2021).
  44. Dean, J. A golden decade of deep learning: Computing systems & applications. *Daedalus* **151**, 58–74 (2022).
  45. Dosovitskiy, A. *et al.* An Image is Worth 16x16 Words: Transformers for Image Recognition at Scale. *arXiv [cs.CV]* (2020).
  46. Dai, X. *et al.* Dynamic head: Unifying object detection heads with attentions. *arXiv [cs.CV]* 7373–7382 (2021).
  47. Chen, Q. *et al.* Group DETR: Fast DETR training with group-wise one-to-many assignment. *arXiv [cs.CV]* 6633–6642 (2022).
  48. Bader, O. N. *Балановский могильник: Из истории лесного Поволжья в эпоху бронзы*. (Издательство Академии наук СССР, 1963).
  49. Bader, O. N. & Khalikov, A. K. *Памятники балановской культуры*. vol. вып. В1-25 (Археология СССР, 1976).
  50. Comsa, E. Mormintele cu ocră din movila II - 1943 de la Ploiesti Triaj. *Thraco-Dacica* **10**, 181–188 (1989).
  51. Dumitrescu, V. *The Neolithic Settlement at Rast:(south-west Oltenia, Romania)*. vol. 72 (BAR Publishing, 1980).
  52. Frînculeasa, A. Podoabe preistorice din materiale vitroase. Descoperiri în cimitirul din epoca bronzului de la Câmpina (jud. Prahova). *Studii de Preistorie* **10**, 189–209 (2013).
  53. Frînculeasa, A., Mirea, P. & Trohani, G. Local cultural settings and transregional phenomena: on the impact of a funerary ritual in the Lower Danube in the 4th millennium BC. *Buletinul Muzeului Județean Teleorman, Seria Arheologie* **9**, 75–116 (2017).
  54. Frînculeasa, A., Preda, B., Simalcsik, A. & Negrea, O. Peisaje și contexte actuale: un tumul de pământ cercetat în localitatea Coada Izvorului, județul Prahova/Present landscapes and contexts: a burial mound excavated at Coada Izvorului, Prahova County. *Materiale și cercetări arheologice* **14**, 77–99 (2018).
  55. Frînculeasa, A. The Children of the Steppe: descendance as a key to Yamnaya success. *Studii de Preistorie* 129–168 (2019).
  56. Frînculeasa, A. Endangered monuments: in rescue of the mutilated and anonymous burial mounds of the steppe. *Revista de Arheologie, Antropologie și Studii Interdisciplinare* **2**, 41–79 (2020).
  57. Frînculeasa, A., Negrea, O., Dîscă, C. & Simalcsik, A. Tumulul II de la Strejnicu (județul Prahova) – o prezentare arheologică și bio-antropologică. *Revista de Arheologie, Antropologie și Studii Interdisciplinare* **3**, 67–104 (2021).
  58. Frînculeasa, A. *et al.* Ritualul Iamnaia și persistențe locale în prima jumătate a mileniului al



- III-lea (complexe funerare cercetate în anul 2021 în nordul Munteniei). *Revista de Arheologie, Antropologie și Studii Interdisciplinare (RAASI)* 127–165 (2022).
59. Gadzyackaya, O. S. *Памятники фатьяновской культуры: Ивановско-Горьковская группа*. vol. 1 (Наука, 1976).
  60. Gymashian, S. V. Новые памятники каменного века Караби-Яйлы. in *Древности степного причерноморья и кыма 4* (eds. Toshchev, G. N., Sharovalov, G. I. & Mikhailov, V. D.) 3–9 (Запорожский Государственный Университет, 1993).
  61. Ivanova, S. V. & Toshchev, G. N. ‘Буджанские Банки’ как маркеры: транскультурный и трансрегиональный аспект 1. *ССПК* 18, (2015).
  62. Костылева, Е. Л. & Уткин, А. В. *Нео-энеолитические могильники Верхнего Поволжья и Волго-Окского междуречья*. (Таус, 2010).
  63. Krainov, D. A. *Памятники фатьяновской культуры: Московская группа*. vol. 1 (Изд-во Академии наук СССР, 1963).
  64. Krainov, D. A. *Памятники фатьяновской культуры: Ярославско-Калининская группа*. (Изд-во ‘Наука’, 1964).
  65. Lougas, L., Kriiska, A. & Maldre, L. New dates for the Late Neolithic Corded Ware Culture burials and early husbandry in the East Baltic region. *Archaeofauna* 16, 21–31 (2007).
  66. Papas, L. *et al.* Dynamic changes in genomic and social structures in third millennium BCE central Europe. *Sci Adv* 7, (2021).
  67. Rosetti, D. V. Movilele funerare de la Gurbănești (r. Lehliu, reg. București) / Les tumulus funéraires de Gurbănești. *Mater. și cercet. arheol.* 6, 791–816 (1959).
  68. *Древности Степного Причерноморья и Кыма II*. (Запорожский государственный университет, Запорожский областной краеведческий музей, 1991).